

Numerical Algorithms for Precise Calculation of Surface Movement in 3-D Topography Simulation

F. A. Leon, S. Tazawa*, K. Saito*, A. Yoshii*, and D. L. Scharfetter
Intel Corporation, Santa Clara, California, U.S.A.
*NTT LSI Laboratories, Atsugi-shi, Kanagawa, Japan

As topography simulation becomes increasingly important for ULSI technology development, the numerical algorithms for movement of the surface during etch, deposition and oxidation simulation require deeper examination. In this paper, two new fundamental algorithms for 3-D surface movement are presented. First, the "characteristic wavefront" method provides highly accurate 3-D vertex movement for vertices with an arbitrary number of adjacent planes, especially for the difficult case of sputter etch. When a vertex is formed from four or more adjacent planes, it is clear that those planes may not have a unique intersection after movement. Thus, previously reported 3-D vertex movement algorithms [1,2], have had simplifying assumptions. Because the characteristic wavefront method treats the case of four or more planes with no simplifying assumptions, it is both highly accurate by itself and can also serve as an important accuracy test. The second algorithm, the "swept solid" method, treats the problem resulting from a growing or etching surface colliding with itself, forming a self-intersecting structure ("loop"). By using basic Boolean set operations, this method rigorously avoids loop formation. The algorithm reported here treats the technologically important case of simultaneous etch and deposition. These two methods have been implemented in the 3-D topography simulation program THUNDERBIRD [2].

Sputter etch is modeled as a surface orientation dependent etch rate; the examples demonstrated here use the functional form $v = (B + C \sin^2 \theta) \cos \theta$, where v is the normal velocity. The evolution of a surface according to an angle dependent rate function has been shown to be given by the following characteristic equation [3] (where $g = v / \cos \theta$):

$$\frac{dx}{dt} = -\frac{\partial g}{\partial \theta} \cos^2 \theta \cos \phi + \frac{\partial g}{\partial \phi} \cot \theta \sin \phi \quad \frac{dy}{dt} = -\frac{\partial g}{\partial \theta} \cos^2 \theta \sin \phi - \frac{\partial g}{\partial \phi} \cot \theta \cos \phi \quad \frac{dz}{dt} = \frac{\partial g}{\partial \theta} \sin \theta \cos \theta - g$$

Looking at the 2-D case first, Fig. 1 shows a 2-D convex corner representing a vertex and its neighboring edges in a surface representation. Fig. 1 also shows the characteristic trajectories for all the orientations included in the vertex as well as for all points on the adjacent edges. We call the locus of trajectory endpoints the "characteristic wavefront." Fig. 2 shows the same for a concave corner. If we choose a direction of propagation for the vertex, the propagation distance is given by the farthest intersection with the characteristic wavefront (convex case), or the closest intersection (concave case). Alternatively, consider the topology of the characteristic wavefront. The intersection of the characteristic wavefront with itself divides the wavefront into "valid" and "invalid" sections. The section of the divided wavefront connected to the wavefront far from the vertex must be valid. If a movement direction is chosen as a ray, the intersection of that ray with the valid characteristic wavefront gives the magnitude of movement.

For the 3-D case, the first step is to construct characteristic wavefronts for each edge separately (omitting trajectories from the vertex), in an analogous way to the 2-D case (see Fig. 3). Then, taking two edges at a time, intersections between wavefronts are determined, and the wavefronts divided into valid and invalid sections; the third step of Fig. 3 shows the resulting "valid" portion of the wavefront. A plane of interest is chosen which includes the vertex movement direction. This plane now defines a 2-D problem, in which the characteristic wavefront is formed from intersections of the wavefronts for each edge with this plane, and from the trajectories emanating from the vertex (final step of Fig. 3).

The swept solid algorithm is first explained in a 2-D analogy (Fig. 4). The growing surface is modified one segment at a time, by constructing "swept solids" and performing union operations with the new solid under construction. The representation is always a consistent, non-self-intersecting solid model. For the 3-D case, in which the surface is composed of triangles, the swept solids are constructed as shown in Fig. 5. Note that because points A, B, A', and B' are not necessarily co-planar, the quadrilateral ABB'A' is divided by the edge AB' so that the swept solid is consistent. The union operations are performed on the swept solids one at a time, as in the 2-D case. For the case of etching, difference operations are used instead of union operations.

The case of simultaneous deposition and etch is illustrated in 2-D. "Temporary swept solids" for etch and deposition are defined as shown in Fig. 6. Now, look at the deposition swept solid for face i , defined as $D(i)$. The algorithm (see Fig. 7) for the construction of $D(i)$ is shown below:

$$D(i) = TD(i) - O; \text{For all neighbors } n: D(i) = D(i) - TE_n(i)$$

where O is the original solid, $TD(i)$ is the temporary deposition swept solid for face i , and $TE_n(i)$ is the temporary etch solid for face n which is a neighbor of i . For the etch swept solid, the corresponding algorithm is:

$$E(i) = TE(i) \cap O; \text{For all neighbors } n: E(i) = E(i) - TD_n(i)$$

After the etch and deposition solids are made, differences and unions are taken, respectively, with the original solid.

Acknowledgments

The authors acknowledge useful discussions with Mr. S. Matsuo and Drs. J. Mar, E. Arai, A. Ishida, and K. Hirata.

References

- [1] E. Scheckler et al., Symp. VLSI Technol. Dig., p.97, May 1991.
- [2] S. Tazawa et al., IEDM Technical Digest, December 1992.
- [3] I. V. Katardjiev, J. Vac. Sci. Technol. A 6(4), Jul/Aug 1988.

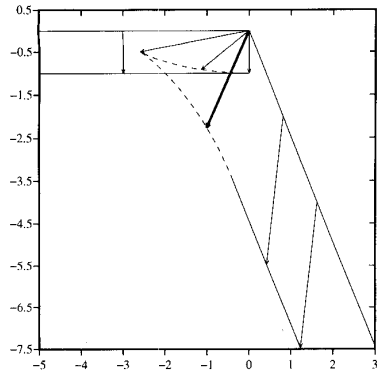


Fig. 1 2-D Convex Case

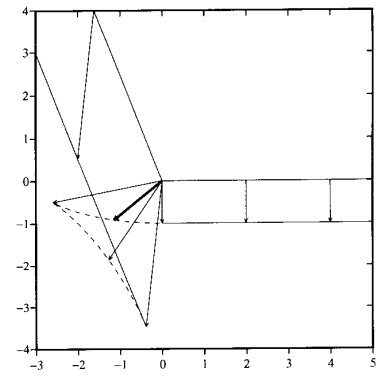


Fig. 2 2-D Concave Case

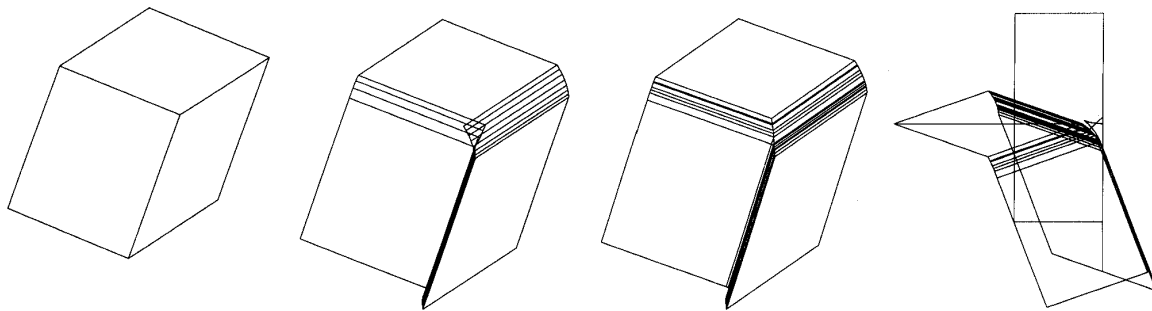


Fig. 3 3-D Characteristic Wavefront Method

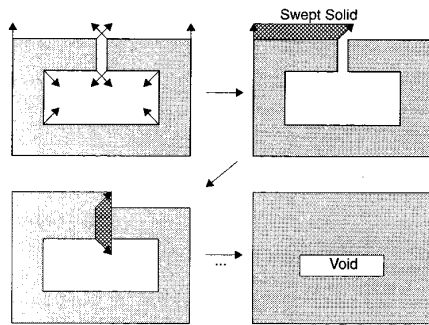


Fig. 4 2-D Swept Solid Method

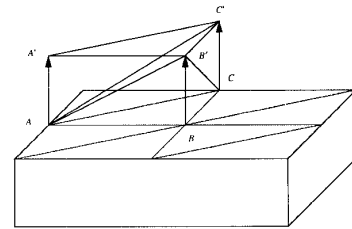


Fig. 5 3-D Swept Solid

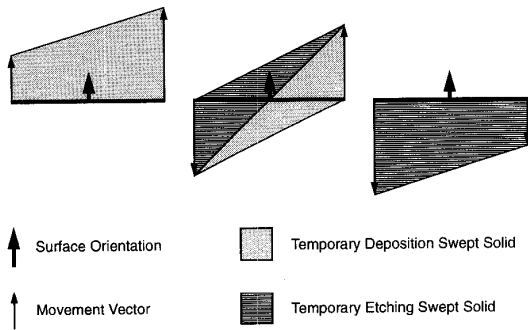


Fig. 6 Definition of Temporary Swept Solids

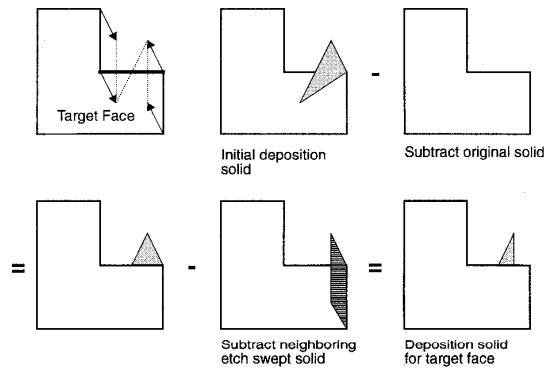


Fig. 7 Creation of Deposition Swept Solid